



EARTH & PLANETARY SCIENCE LETTERS



This article was published in an Elsevier journal. The attached copy is furnished to the author for non-commercial research and education use, including for instruction at the author's institution, sharing with colleagues and providing to institution administration.

Other uses, including reproduction and distribution, or selling or licensing copies, or posting to personal, institutional or third party websites are prohibited.

In most cases authors are permitted to post their version of the article (e.g. in Word or Tex form) to their personal website or institutional repository. Authors requiring further information regarding Elsevier's archiving and manuscript policies are encouraged to visit:

<http://www.elsevier.com/copyright>



ELSEVIER

Available online at www.sciencedirect.com

ScienceDirect

Earth and Planetary Science Letters 260 (2007) 419–431

EPSL

www.elsevier.com/locate/epsl

Combining CSD and isotopic microanalysis: Magma supply and mixing processes at Stromboli Volcano, Aeolian Islands, Italy

D.J. Morgan^{a,c,d,*}, D.A. Jerram^a, D.G. Chertkoff^a, J.P. Davidson^a, D.G. Pearson^a,
A. Kronz^b, G.M. Nowell^a

^a Department of Earth Sciences, University of Durham Science laboratories, South Road, Durham DH1 3LE UK

^b Geowissenschaftliches Zentrum Göttingen, Goldschmidtstraße 1-3, 37077 Göttingen, Germany

^c Laboratoire Géodynamique des Chaînes Alpines, UMR5025, Université Joseph Fourier, 1381 rue de la piscine, 38400 Saint Martin D'Hères, France

^d School of Earth and Environment, Earth Sciences building, University of Leeds, LS2 9JT UK

Received 31 May 2006; received in revised form 16 May 2007; accepted 20 May 2007

Available online 26 May 2007

Editor: C.P. Jaupart

Abstract

Integrating isotopic microanalysis with other analytical techniques creates powerful new methodologies for understanding the evolution of rock samples at the sub-grain scale. Here we present Crystal Size Distribution (CSD) data for a 26,000 year old sample from Stromboli Volcano and accompanying isotopic microanalysis of the phenocrysts. A technique, called the ICSD plot, is introduced which given stated assumptions allows the integration of both sets of data to generate timelines of isotopic evolution through the volcanic system. The combined approach is powerful, allowing investigation of the magma supply, mixing, crystallisation and contamination processes prior to eruption of a volcanic sample. For Stromboli Volcano, the combined analysis suggests that the change in magma type following a cone collapse took roughly five years to complete, similar to the timescale of changes seen in recent decades.

© 2007 Elsevier B.V. All rights reserved.

Keywords: CSD; isotopic microanalysis; Micromill; microdrill; Stromboli; ICSD

1. Introduction

Isotopic microanalysis in geochemistry has undergone rapid development in recent years (Davidson and Tepley, 1997; Wolff and Ramos, 2003; Ramos et al., 2004; Francalanci et al., 2005; Ramos et al., 2005), detailing magmatic processes through information stored at the sub-grain scale. Placing timescale constraints on this data is vital to reveal important information concerning recharge dynamics at volcanoes, and thus aid predictive

modelling. Our method is to combine isotopic microanalyses with textural analysis (Crystal Size Distribution, CSD) (Marsh, 1988), another rapidly-evolving quantitative technique (Higgins, 2000; Zieg and Marsh, 2002; Boorman et al., 2004; Mock and Jerram, 2005). Such combined analysis allows a greater understanding of the evolution of rock samples at the sub-grain scale in the context of the whole-rock texture (Muller, 2003; Turner et al., 2003; Morgan and Jerram, 2006; Jerram and Kent, 2006).

Here we present microsampling and CSD datasets which we discuss and integrate in order to gain insights into magma mixing processes through time. The method

* Corresponding author.

E-mail address: d.j.morgan@leeds.ac.uk (D.J. Morgan).

provides information on the growth history of crystals through time (Marsh, 1998) as well as quantifying the contribution of xenocrysts to the whole rock. Mass balance of the results gives a perspective on the whole-rock isotopic ratio as a mixture of several components. We demonstrate the technique on a sample from the Vancori period (26 ka) of Stromboli Volcano (Hornig-Kjarsgaard et al., 1993), compositionally similar to the present system (Francalanci et al., 1999; Francalanci et al., 2004; Francalanci et al., 2005). Our results suggest that isotopic components and processes during the Vancori period were similar to those seen at the present day and operated over similar timescales. This shows that the Vancori period volcanics may be used as a proxy for possible future behaviour at Stromboli, and may therefore lead to the construction of better hazard models.

2. Methods

The present study employs both a textural analysis and microsampling approach. In each case a detailed understanding of the rock texture and crystal population is of paramount importance. Below, we introduce both techniques, then present the key samples used for this study.

2.1. CSD analysis

The 3D crystal population for a volcanic rock can be quantified by looking at CSD data which considers the population density of different crystal sizes. CSD analysis commonly looks at crystal sizes taken from 2-dimensional thin sections, to which geometric (Higgins, 1994a,b; Higgins, 2000; Morgan and Jerram, 2006) and stereological (Higgins, 1994a,b, 2000) corrections are applied to access the true 3D CSD. Data are presented as log crystal abundance per unit volume against crystal long axis measurement (Marsh, 1988; 1998). Such graphs contain information on crystal growth rate and growth time. Assuming simple, linear crystal growth, the CSD will be a straight line, the gradient of which is related to the crystal growth rate and the time that has passed during crystallisation (Marsh, 1988; Marsh, 1998; Zieg and Marsh, 2002; Boorman et al., 2004). Using experimentally-measured growth rates (Cashman, 1990; Jerram et al., 2003; Armienti et al., 2007), magma crystallisation timescales can be determined (Marsh, 1988; Cashman and Ferry, 1988; Cashman and Marsh, 1988; Cashman, 1990; Jerram et al., 2003). Such timescale information is of critical importance in the drive to understand magmatic processes for predictive

purposes. Examples of crystal populations where CSD plots are kinked/curved are the result of more complicated processes such as the mixing of crystal populations (Marsh, 1988; Cashman and Ferry, 1988; Cashman and Marsh, 1988; Cashman, 1990; Jerram et al., 2003) signifying key changes in the timeline of the magma system.

2.2. Isotopic microanalysis

Using high-resolution sample excavation (micro-mill/drill) and laser techniques it is possible to attain high quality *in-situ* isotopic microanalysis from within individual crystals (Davidson and Tepley, 1997; Ramos et al., 2004; Charlier et al., 2006). With the micro-milling technique, described in more detail below, the quality of the data is enhanced because possible elemental interferences can be eliminated through the separation chemistry before analysing for isotopes, leading to higher precision. With isotopic microanalysis the range of isotopic variation within crystals and between different crystals from the same population can be quantified.

In examples where isotopic heterogeneity can be shown at the sub-grain scale, such isotopic variations within and between crystals have been related to mixing between different magmas, recharge events in magma bodies and contamination (Davidson and Tepley, 1997; Gagnevin et al., 2005b). The time aspect of isotopic information is, for many crystal phases, not well-constrained at the grain/sub-grain scale. Ingrowth effects of radiogenic isotopes are of use only if time elapsed since eruption is small relative to the timescale of process under investigation, as post-eruptive ingrowth will dominate pre-eruptive records. In looking at the high temperature residence through diffusion, isotopic data, due to small variations (third decimal place or smaller), large data points (>30 μm) and relatively large uncertainties are difficult to model (Gagnevin et al., 2005b,a), and radioactive isotopes are generally so low in abundance that they cannot be measured *in-situ* with current technology other than in the most enriched phases, such as zircon for U-series analysis (Charlier et al., 2005). Even then, timescale information is only accessible for samples within a certain age range as the short timescale information recorded by U-series disequilibria decay to within measurement uncertainty of secular equilibrium within seven half-lives of the daughter isotope. Therefore, an external source of specifically short-term pre-eruptive timescale information is needed that can be related to the crystal isotopic record.

2.3. Samples

To compare CSD and isotopic microanalysis, we studied a lava (STR46) from the Lower Vancori period (26 ka) of Stromboli Volcano in the Aeolian Islands (Hornig-Kjarsgaard et al., 1993). CSD data were obtained by tracing 1465 plagioclase crystal outlines from a high-resolution scan of a thin section. Processing was performed using ImageJ® and Microsoft® Excel®. The raw, two-dimensional CSD data are shown in Fig. 1a. A mean crystal shape for the whole feldspar population was determined to be 1:2.8:4 using *CSDslice* (Morgan and Jerram, 2006) and this shape was used with the v.1.3 *CSDcorrections*® software (Higgins, 2000) to calculate the 3D CSD from the 2D data (Fig. 1b).

2.4. Crystal selection for microanalysis and initial inspection

Plagioclase crystals were sampled using a New Wave® MicroMill® for the extraction and isotopic analysis of strontium at the nanogram level (Charlier et al., 2006). For microsampling, large crystals were selected on the grounds that they have a longer magmatic history and provide more material, particularly at the crystal rim. Crystals were also selected against further criteria:

1. well-defined zonation for ease of drilling
2. zonation that persists into the crystal core
3. zonation across at least four crystal faces, at least two of which are parallel.

The last constraint here is to identify sections that are cut as close to the centre of the crystal and perpendicular to one of the major crystal axes.

2.4.1. Crystal STR461

The largest crystal in the first thin section, STR461 (Fig. 2a) shows a resorbed core, a broad, darkened zone packed with melt inclusions, and a clear rim. The strong resorption of the core region suggests that it may have been inherited.

2.4.2. Crystal STR462

A glomerocryst, STR462 (Fig. 2b) has a core comprised of three separate crystals, distinguishable with a petrological microscope. The rim zone, is however consistently grown around all three cores, suggesting that STR462 was remobilised as a glomerocryst prior to rim growth. Therefore a two-stage (at least) history for this crystal can be inferred directly from its appearance in

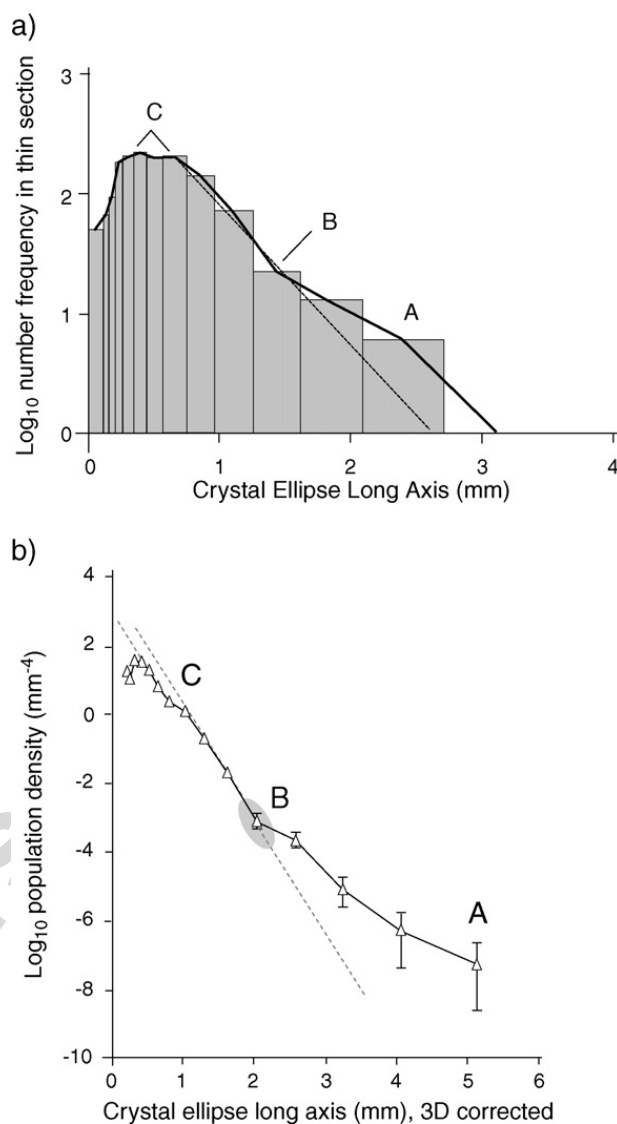


Fig. 1. a). 2D-CSD data for sample STR46. The CSD consists of two linear regions with a noticeable kink at ~ 1.5 mm crystal size. b). 3D CSD, using *CSDcorrections* (Higgins, 2000) and a crystal shape of 1:2.8:4. Region A is the tail of the CSD, and shows an over-abundance of large crystals relative to an extrapolation through the linear region of smaller crystals (dashed line). Region B (shown with uncertainty by the grey ellipse) is the location of a kink in the curve, where the linear population and the larger cores start to interact. Region C shows a dog-leg in the CSD profile where there is an offset followed by a return to the same gradient as seen in the larger crystals.

thin section. For isotopic analysis, only the largest, left-hand core was analysed.

2.4.3. Crystal STR463

STR463 (Fig. 2c) is a strongly zoned crystal sectioned through the crystal centre. Due to the high clarity of the zonation in this crystal, high-resolution drilling was possible despite the smaller crystal area than STR461. This crystal appears to be very simple and although it displays various zones of resorption – showing as dark

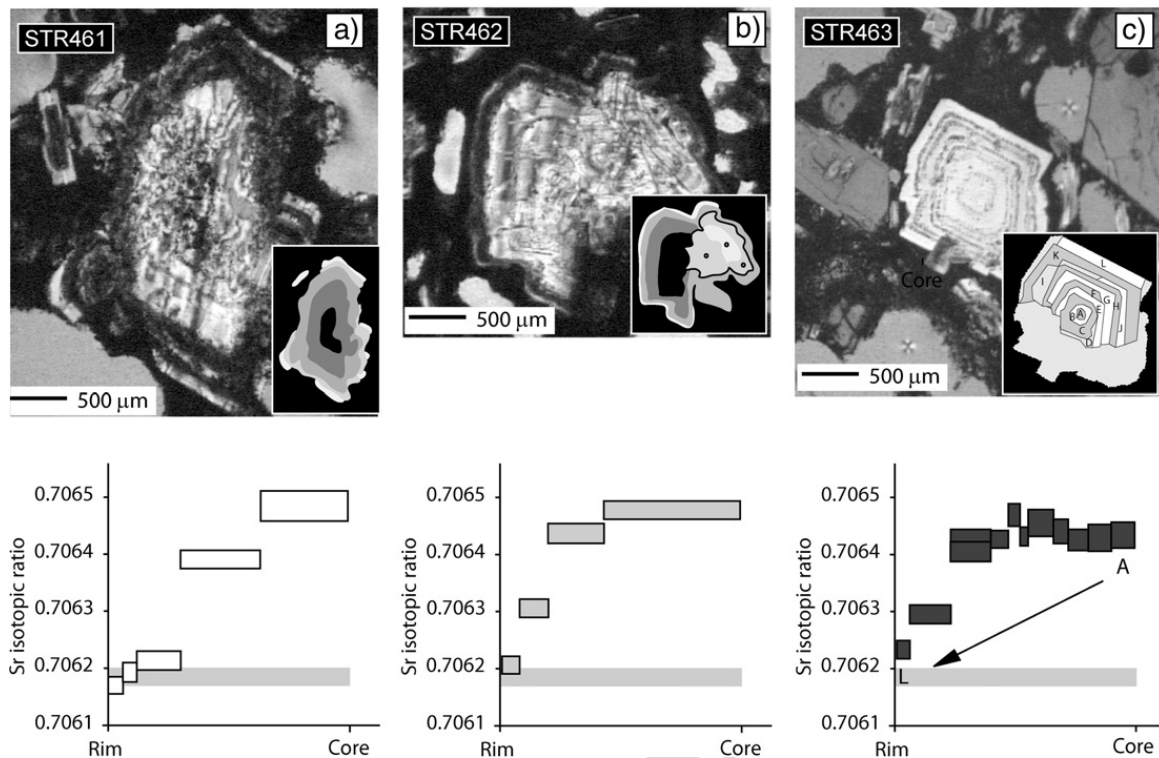


Fig. 2. a–c. The upper part of this figure shows transmitted-light photomicrographs of crystals STR461–3 prior to drilling and the drilled zones (insets). The lower part of the figure shows the core-to-rim isotopic variation in each case. Box widths correlate with the size of drilled zones, as a fraction of the core-to-rim distance, and box heights show two-sigma uncertainty. The groundmass glass isotopic ratio is indicated by the horizontal grey bar.

bands of melt inclusions – these seem relatively minor compared to those of crystals STR461 and STR462.

In addition, a groundmass crystal STR46GM and the groundmass glass were also analysed.

Results are listed in Table 1 with two-sigma uncertainties including propagated internal and external uncertainties governed by 8 NBS987 standard measurements (6 ng load) run with the samples.

3. Interpretation of CSD data

Taken in isolation, the 3D-corrected CSD of Fig. 1b shows a well-constrained curve with three main regions of importance. Region A is the tail of the CSD, and shows an over-abundance of large crystals relative to an extrapolation through the linear region of smaller crystals (dashed line). This excess exists outside of the range of plausible uncertainty shown by the uncertainties on the larger crystal abundances, and therefore is real. The CSD tail seems curved, but uncertainties are too large to ensure a non-zero curvature. Region B (grey circle) is the location of a kink in the curve, where the larger crystals start to interact with the linear region representing the simple population of smaller crystals. The exact position of the kink is somewhat uncertain; however, by binning the data in different size bins, the magnitude of the

binning effect on kink location can be investigated. This shows that the kink originates in the horizontal range shown by the grey ellipse, although vertically the kink is well-constrained to lie on the dashed line by the small uncertainties on the data points. Region C is interesting as it shows a dog-leg in the CSD profile where there is a small offset separating two regions of the same gradient. Due to the high abundance of crystals in this size range and the close spacing of the bins, this step is significant and well-defined despite the apparent small magnitude. Such a step could originate due to a transient increase in growth rate due to an episodic degassing process. Importantly, both these deviations from a simple straight CSD profile are also visible in the unprocessed 2D CSD shown in Fig. 1a, and are therefore not due to the reprocessing of the data to the 3D CSD plot. In Fig. 1a, the dog-leg, C, is quite visible as a double peak and the tail of the distribution and the kink are also represented. In the processed data the predicted largest crystals in the population are bigger than those present in the 2D section, as the 3D data accounts for the section effects on the size range and morphology of the crystals.

The kink in the crystal population could result from a mixed population of crystals (Marsh, 1988; Cashman and Ferry, 1988; Cashman and Marsh, 1988; Cashman, 1990; Jerram et al., 2003), with more than the expected

Table 1

Crystal/ sample	87 Sr/86 Sr ratio	Uncertainty (2s)	Fractional distance	
<i>STR461</i>				
A	0.706484	2.3E-05	0.00	Core
B	0.706390	1.1E-05	0.37	
C	0.706213	1.3E-05	0.70	
D	0.706191	1.2E-05	0.88	
E	0.706171	9.0E-06	0.94	Rim
<i>STR462</i>				
A	0.706478	1.1E-05	0.00	Core
B	0.706437	1.3E-05	0.57	
C	0.706306	1.2E-05	0.80	
D	0.706207	9.0E-06	0.92	Rim
<i>STR463</i>				
A	0.706436	2.0E-05	0.00	Core
B	0.706431	2.1E-05	0.10	
C	0.706427	1.3E-05	0.20	
D	0.706442	1.8E-05	0.28	
E	0.706457	2.0E-05	0.34	
F	0.706434	1.2E-05	0.45	
G	0.706471	1.4E-05	0.48	
H	0.706429	1.1E-05	0.53	
I	0.706407	1.3E-05	0.60	
J	0.706429	1.2E-05	0.60	
K	0.706297	1.0E-05	0.77	
L	0.706235	1.1E-05	0.95	Rim
Groundmass glass	0.706184	1.50E-05		Groundmass

number of large crystals in the population due to the inclusion of more crystals in this size fraction at some stage. If we mix two or more crystal populations how valid is it to use one shape when processing the data from 2D to 3D? Here we have tested this using *CSDslice*; by passing only the larger crystals to the *CSDslice* algorithms we can determine if there is a significant component of differing morphology. Although this process is somewhat artificial as we are also removing small sections through large crystals at each iteration of this process, it at least serves to interrogate the existence of significant shape variations in the data. The results are compiled in Table 2, where R^2 denotes the coefficient of correlation between binned abundance of length–width measurements of fitted ellipses in the data to those of a model data set. Note that the *CSDslice* routine (as with CSD analysis itself) becomes unreliable below a sample size of ~ 250 crystals (Mock and Jerram, 2005; Morgan and Jerram, 2006). In this study, however, the returned crystal morphology is remarkably stable at 1:2.8:4, even down to crystal populations of below 100. Only in the last step, when only 50 crystals are considered, does the confidence collapse, at a pop-

ulation density which is statistically not valid (Mock and Jerram, 2005; Morgan and Jerram, 2006), Fig. 3. While this is the fraction in which all of the larger crystals that were microsampled happen to lie, for the vast majority of the population, the shape estimate is robust. In studies where the true 3D CSD is known it has been shown that corrected 2D data using an average shape estimate, such as that presented here, successfully reproduced the true 3D curve even when significant shape variation was present (Mock and Jerram, 2005). With the extremely well sampled (1465 crystals) population in this study we can show that there is a significant deviation from a straight curve at approximate long axis size of 2–2.5 mm in the corrected 3D CSD.

4. Isotopic results

The isotopic work shows that there is a significant shift in isotopic ratios from core to rim across all three crystals, with cores showing elevated isotopic ratios and rims of lower ratios approaching that of the groundmass glass (Fig. 2). This is consistent with the concept of crystal core inheritance and a subsequent common overgrowth rim. The crystal cores appear to have at least two different origins, as the core of STR463 cannot be reconciled with those of STR461 and STR462, although the progression of isotopic ratios in the crystal rims appears to be entirely common to all three crystals, at least to start with. Crystal STR463 does not develop a rim in complete isotopic equilibrium with the host glass, suggesting that the rim is either very thin ($<30 \mu\text{m}$), or that the crystal was actively removed from the crystallising system at some point prior to the eruption. To address the crystal histories in more detail:

- Crystal STR461 shows a quite simple evolution; a core forms which is then subjected to changing isotopic ratios which are recorded in successive growth zones up until the point of eruption. The rim zone of STR461 is in equilibrium with the groundmass glass

Table 2

Number of crystals	x	y	z	R^2
1465	1	2.8	4	0.8835
1000	1	2.8	4	0.8877
500	1	3.2	4	0.9002
400	1	3.2	4	0.9160
300	1	3.2	4	0.9030
200	1	2.7	4	0.8587
150	1	3.2	4	0.8473
100	1	2.7	3.8	0.8474
50	1	2.6	4	0.6966

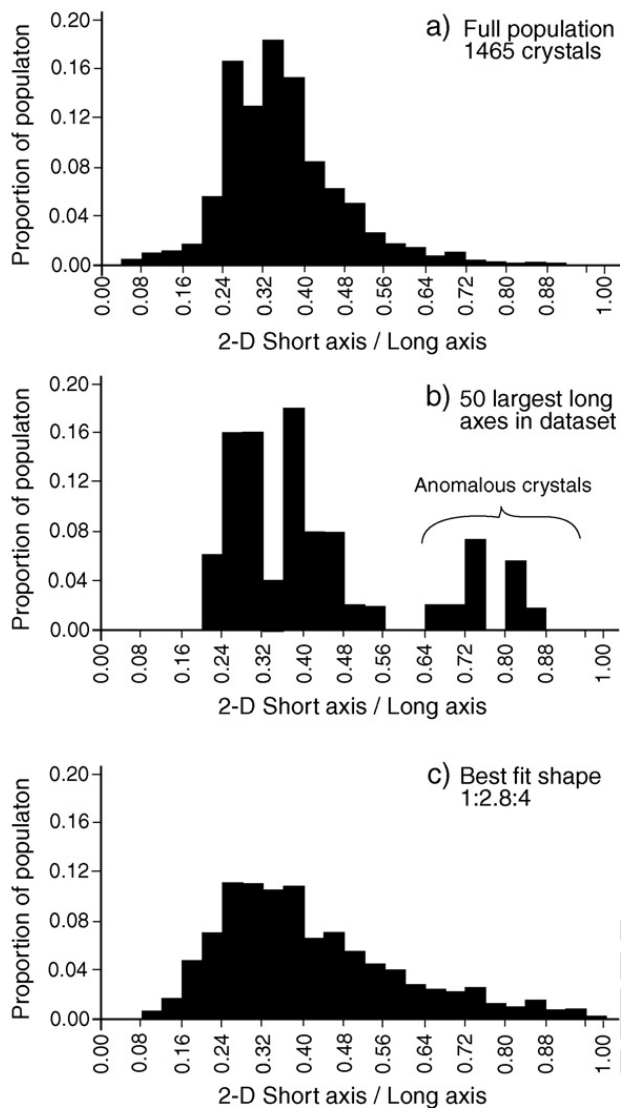


Fig. 3. Graph of binned short-axis to long axis ratios *versus* frequency as a proportion of the population, presented as a connected. Here, the 50 largest crystals (defined by the long-axes of fitted ellipses) within the 1465-crystal assemblage of STR46 are shown with a dashed line. The envelope for the full population of 1465 fitted ellipses (grey) and the best-fit shape of 1:2.8:4 (solid line). Note that there is a population of 10 crystals with high short-axis to long-axis ratios in the range 0.6–0.9. These are an excess over the predicted 0–1 crystals according to the dominant crystal shape, and suggest that the very largest crystals may have a different, more equant shape than that possessed by the majority in the thin section.

suggesting that it records the complete history of isotopic variation in the magma. However the strong resorption of the crystal core suggests that there is a hiatus and that the core may have been derived from a pre-existing cumulate.

- STR462 starts as three separate crystals, with a similar isotopic ratio to the crystal core of STR461, which merged to form a glomerocryst, perhaps in a cumulate mush zone (Jerram et al., 2003) in order to allow adcumulus growth to join the three cores. This

glomerocryst is subsequently remobilised into the convecting magma in order to form the coherent, consistent-thickness rim mantling all three cores.

- STR463 on the other hand is a single crystal which does *not* in thin section display obvious multiple cores or evidence of cumulate history but which *isotopically* reflects a complex evolutionary path. The core of STR463 shows an isotopic ratio distinctly different from the cores of STR461 and STR462 and yet the same progression of isotopic change towards the rim as both of these crystals. Therefore, the core has a different origin and the rim a common origin with STR461 and STR462. The rim-most zone of STR463 retains a higher isotopic ratio than that of STR462, which suggests that STR463 is missing more of the immediate pre-eruptive record at the rim than STR462 and STR461, and therefore left the magma system earlier during the stages of isotopic change in the surrounding magma.

5. Linking the two data sets — isotopic timelines and the ICSD plot

CSD data represent the overall 3D crystal population and the desired information concerning time and growth rate, and the isotopic data represent a change in the isotopic composition of the magma supply to the volcano. Thus linking the two data types is desirable to investigate time aspects of isotopic changes and effects on crystal growth history caused by magma source change. Employing the techniques presented here, the isotopic variation through time can be examined and individual crystals pinned onto a qualitative timeline linking them to the CSD population.

In order to have a more quantitative base, the re-processed, 3-D CSD information is used; this particular way of exhibiting the data has components related to growth and nucleation rate and hence contains time information. In order to be able to link the two data sets, several criteria must be met:

1. The sample must obey the rules for quantitative CSD analysis. These include:
 - a. The population of crystals sampled exceeds 250 in number
 - b. Crystal morphology, and any foliation or fabric are taken into account
2. There must be a continuous, straightforward change in the measured isotopic ratios, derived from the system as a whole, which allows crystals to be compared.
3. Crystal zoning is roughly concentric on a fixed centre.

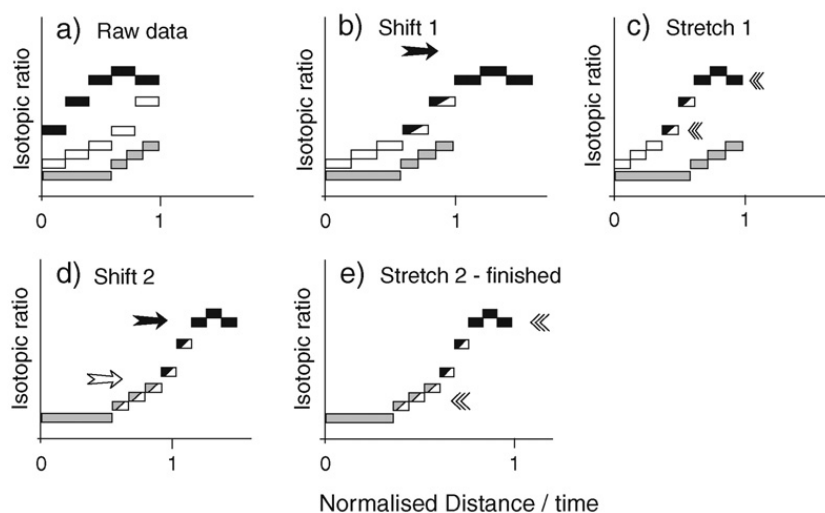


Fig. 4. a–e). Schematic, simplified representation of the stretch-and-shift method used to fit the different isotopic profiles together in order to generate an isotopic timeline. a) For each crystal, isotopic ratio is plotted against distance from rim normalised to the entire core–rim distance. b–d) Data are overlaid to form a complete, single timeline using stretch and shift transformations along the x -axis. e) A final renormalisation gives an isotopic progression derived from multiple crystals that represents the isotopic evolution that would be seen in a crystal that was forming at a uniform rate over the entire crystallisation history of the magma represented by the analysed crystals.

In addition the following assumptions are made:

1. That the microsampled crystals:
 - a. Being the largest crystals in the sample, represent, altogether, the most complete record of crystallisation.
 - b. Are completely sectioned through the centre of the crystal
 - c. Are not wholly xenocrystic but have been interacting with the magma over a significant time period
2. That crystal cores and rims were created by comparable processes operating at similar rates
3. Crystals do not contain multiple growth hiatuses.

We shall return to the validity of these criteria and assumptions for the Stromboli sample in the Discussion section.

5.1. Linking methodology

The isotopic data can be linked to the CSD in two stages, a normalisation followed by a comparison step.

5.2. Stage 1 — normalisation

Analyses are presented with crystal rim as zero distance, since it represents the closest point to zero time since growth. In theory, any crystals growing up to the point of eruption should record a common isotopic ratio in the grain rim. Assuming a linear growth rate, this first stage of the linking procedure simply consists of pre-

senting the data in the correct direction and normalising each crystal to its maximum radius, as already shown for each crystal in Fig. 2a–c. The normalisation accounts for the bulk of the orientation and crystal shape effects on traverse length, since crystals have already been selected on the basis of centre sectioning. The micro-sampling method also does not lend itself to conventional core–rim traverses as for sample volume reasons microdrilling is extended along other crystal faces at different radial distances to the crystal centre, meaning that in different directions within the crystal traverses have different lengths.

5.3. Stage 2 — comparison

If all crystals share a simple growth history, then crystal rims should all have a common $^{87}\text{Sr}/^{86}\text{Sr}$ ratio. However, in many volcanic systems, including the one discussed here, crystals do *not* share a simple growth history (Wallace and Bergantz, 2002; Wallace and Bergantz, 2004). The possible complexity of such paths is high; indeed, in terms of major element zonation, comparing different crystals is difficult (Wallace and Bergantz, 2002; Wallace and Bergantz, 2004), although isotopic zonation is usually more consistent between crystals (Tepley and Davidson, 2003), suggesting different controls. Consistent with previous work (Tepley and Davidson, 2003), we initially assume a low complexity level for the isotopic data, with crystals representing large periods of crystallisation time with possible hiatuses at either end of a continuous crystallisation period. Coping with even such simplified

variation is dependent on the linear growth rate assumption, where time is proportional to crystal radius. Under this scenario, crystals may be stretched by simple factors, accounting for sectioning orientation and different growth times, and shifted along the x -axis to account for crystallisation in different time periods. A simplified process is illustrated schematically in Fig. 4(a–e). Initially, non-dimensionalised data for all crystals are displayed together (4a). Looking at the traverses, we can overlay the rim of the black traverse with the core of the white traverse (4b), and this is then renormalised to the total distance (4c). We repeat this overlay and renormalisation operation with the white and grey traverses, respectively (4d and 4e).

Upon completion of this process, the x -axis of normalised crystal size becomes an *isotopic timeline*, a useful (but qualitative) piece of data in its own right, and one that can be further compared to the CSD crystal size axis after appropriate scaling, giving an Isotopic-CSD (ICSD) plot. The ICSD plot has, given the criteria and assumptions stated, a *quantitative* significance given a good knowledge of the 3D crystal habit, which can be determined by using a routine such as CSDslice (Morgan and Jerram, 2006) and cross-checked by comparing the

calculated crystal fraction output by CSDcorrections (Higgins, 2000) and that measured; these should agree.

5.4. Application to real data

As might be expected, real data are somewhat more complex. We shall now consider what happens in the case of STR46.

Leaving aside crystal STR463 for the moment, the normalised data for crystals STR461 and STR462 are shown in Fig. 5a. In order to avoid subjectivity, we invoke the second of our criteria:

- That the crystals have shared (at least in part) a common isotopic history
- The isotopic variation was simple and continuous.

Initially considering crystals STR461 and STR462, we work in from the rim, which should be zero age for all crystals. Immediately, a deviation is encountered. Crystal STR462 has a higher $\frac{87}{86}\text{Sr}$ rim-value than STR461, whilst STR461 is in equilibrium with the groundmass glass. Considering groundmass glass as truly zero-age, only STR461 has a zero-age rim. STR462

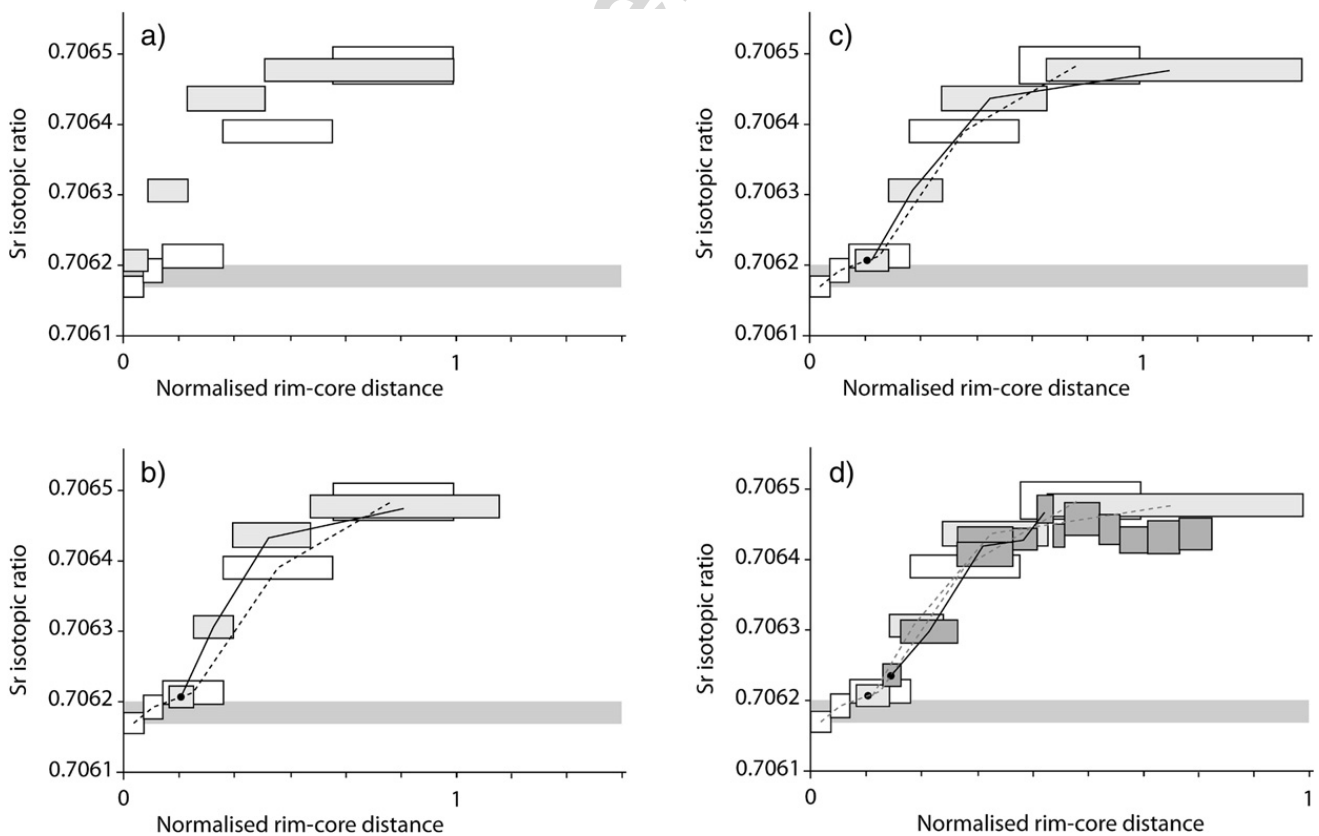


Fig. 5. a–d). Application of the stretch-and-shift procedure to real data. See main text for full explanation.

does not, therefore, have a zero-age rim (at the scale of our isotopic analysis). As the rim, averaged over the whole drilled zone, is older, STR462 must be shifted to the right (towards greater age) until the rim–zone matches the isotopic progression shown by STR461. A line of isotopic progression is drawn through the centre of the data points of STR461 and the data of STR462 shifted right, onto that line. The relatively low number of data points in isotopic microanalysis leads to some difficulties, but the methodology is repeatable and avoids subjectivity. This leads us to Fig. 5b and a tie point (black spot) between STR461 and STR462. Considering later zones, a line drawn through the STR462 data has a steeper gradient than that of STR461. If the isotopic history is a common one, as we assume, then as shown in 5b, the contamination of STR462 is too fast (steep) relative to STR461 and so must occur over a longer period of time. Therefore the data are stretched to the right to bring the lines into closer agreement, shown in 5c. We can repeat this process for crystal STR463, leading to the condition in Fig. 5d. Note that for STR463, the isotopic values of the core region do not agree with those of STR461 and STR462, and so although we can fit the changing isotopic trend for the rimward zones, the core region is not reconcilable with either STR461 or STR462 in an exact sense, and so is not further manipulated. The combined data are then scaled onto the 3D-CSD diagram using the assumption 1a, that the crystals record effectively the entire crystallisation history (and hence the entire range in crystal size), to yield the ICSD diagram (Fig. 6). This shows the isotopic ratio of the

crystal core that is expected for a crystal whose maximum length (in 3D) is given on the x -axis. Note that the crystal growth time runs from right (crystal cores, bigger, older crystals) to left (crystal rims, microcrystals and pre-eruptive growth). As both the CSD and isotopic data have been converted into effective time series, they can be overlaid in this manner; the isotopic data refer to radial size and the CSD to total crystal size – effectively the diameter – although the normalisation of the isotopic timeline (Fig. 5d) onto the CSD scale accounts for the factor of two difference that would be expected.

6. Results of the ICSD

Fig. 6 shows a marked increase in isotopic ratio of the crystal core between model crystal lengths of 0 mm and 2.5 mm. At crystal sizes greater than 2.5 mm, the core ratio reaches an elevated plateau at $\frac{87\text{Sr}}{86\text{Sr}} \approx 0.70645$, although as discussed above there appear to be multiple, distinct core ratios. The onset of the change in ratio (vertical dashed line) correlates loosely with the kink in the CSD between 2 mm and 2.5 mm crystal size. This interpretation is consistent with both data sets.

There are two sets of information that can be extracted from the ICSD plot, the first concerning the crystal zonation for major- and trace-elements and the second concerning the contributions of all crystal zones to the whole-rock isotopic ratio.

6.1. Relationship to crystal zonation

Independently of the CSD results, the evolution curve for the isotopic ratio, the isotopic timeline, can be exploited for examining other aspects of the crystal zonation. The isotopic ratio recorded by a crystal is independent of crystallisation conditions such as temperature, pressure and magma water content, and so when combined across all crystals this provides a relative (not absolute) chronological reference useful for comparing the variability of the major and trace elements across analysed crystals.

Major element patterns derived from anorthite-calibrated backscattered electron images are shown in Fig. 7. Wavelength-dispersive analyses were made of the crystals using a JEOL8900 RL electron microprobe at the University of Göttingen, Germany, and integrated back-scattered electron (BSE) images were taken of the samples. For the three crystals in this study, two were susceptible to having their anorthite contents taken from the BSE image following the method of Ginibre et al. (2002). The third (STR462) exhibited highly complex zonation geometry and cracking which precluded use of

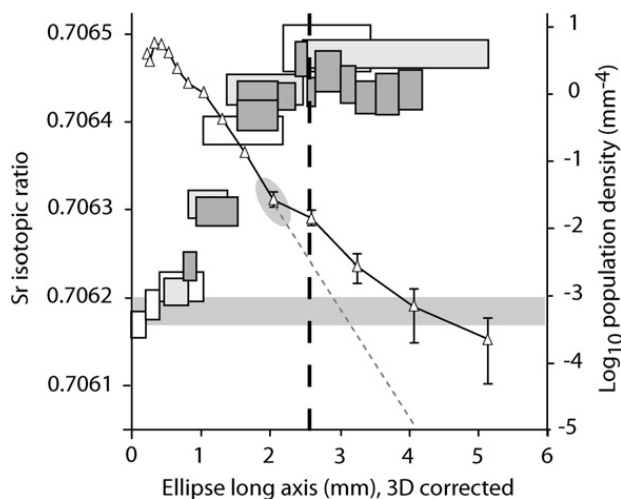


Fig. 6. ICSD plot for STR46. The kink in the CSD (the uncertainty in position of which is indicated by the grey ellipse) occurs coincident with the onset of change in isotopic ratio (strong vertical dashed black line). Uncertainties in the CSD are shown where they are larger than symbol size; boxes show $\pm 2\sigma$ uncertainty on isotopic ratio. The groundmass glass isotopic ratio is indicated by the horizontal grey bar.

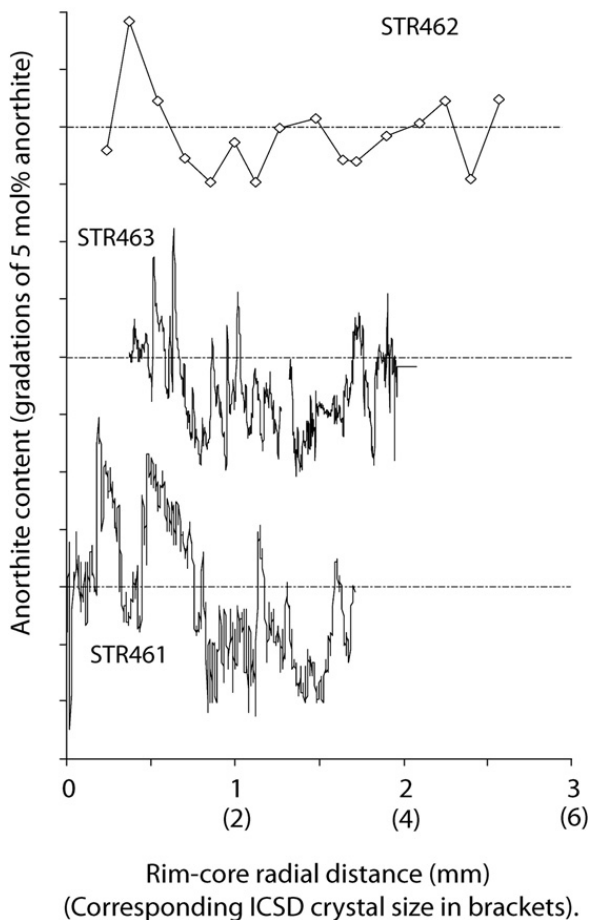


Fig. 7. High-resolution anorthite profiles extracted from accumulated image maps of crystals STR461 and STR463, and a microprobe transect across crystal STR462. All crystal traverses have been scaled according to the suggested crystal size from the isotopic timeline. Dash-dotted lines indicate $X_{An}=0.7$ and tick marks on the vertical axis are 5 mol% anorthite. Note that the crystal zonation does not show any strong correlation between crystals despite a common isotopic ratio evolution.

the image for this purpose; a microprobe traverse is given instead. The crystal traverses shown in Fig. 7 have been scaled to the appropriate position given on the ICSD plot, but separated vertically for clarity. The profiles appear chaotic; any meaningful correlations are not immediately obvious, and detailed analysis would really need a wavelet-based decomposition (Wallace and Bergantz, 2002). Generally speaking, the isotopic ratio does not seem to be correlated to the anorthite content within each crystal, and, to an extent, at least, the records are independent. This is important, in that it shows that major element distributions need not be the same for crystals growing at the same time. Crystal STR463 and STR461 shared parts of their magmatic history (from the isotopic data) and yet diverge in major element contents. The strontium isotope ratio appears to be globally controlled for all crystals, and so there are two plausible explanations for the differences in major

element compositions: Either there are heterogeneous crystallisation environments (with differences in pressure, temperature, water fugacity or major element composition) within the magma chamber, or, major element zonation in plagioclase is a process controlled by local thermodynamic effects. It is not possible to determine the relative importance of each of these possibilities with our current data.

6.2. Checking the ICSD through isotopic mass balance

We can obtain a mass-balance estimate for the isotopic ratio of the whole rock expressed as the sum of its parts by integrating the size bins of the CSD with the isotopic data, fractional abundance and strontium contents of glass and feldspar (by ICPMS and EPMA) and compare this with the measured whole-rock $\frac{87}{86}\text{Sr}$ ratio. This should allow us to determine whether our assumptions are valid within the uncertainty of our analysis.

The strontium content of the feldspars was determined by EPMA on the three crystals analysed for isotopic ratio. The results give a mean Sr content of 1300 ± 434 ppm (2σ , 36 analyses). A glass fraction of 41% and plagioclase crystal fraction of 26% were balanced using a partitioning relation adjusted to yield a whole-rock strontium content of 660 ppm, a feldspar strontium content of 1316 ppm and a strontium content for the glass of 774 ppm (the remaining 33% of the sample is composed of clinopyroxene and olivine, assumed to have negligible Sr contents). The modelled partition coefficient for Sr into plagioclase from melt is 1.7, very close to published estimates from experimental and natural samples (Ewart et al., 1973; Bindeman et al., 1998).

The CSDcorrections program gives a breakdown of the population in size bins, for each of which is also calculated the volume fraction of the sample which they represent. The isotopic ratio expected for any size bin can be calculated, however this will be a mixture of core and rim components, determined by reference to the isotopic evolution line, and whose exact contribution has to be worked out for each radial division, each “shell” of the crystal bin. Therefore the smallest crystals are composed only of rim material, crystals in the middle of the range having zones of several, graded isotopic values, and only larger crystals contain core-type material at their centres. Even in this case, the volume of even a thin rim is large with respect to the crystal core, and the core material introduces only relatively minor deviations in the bulk crystal ratio from that of groundmass glass.

Integrating across all size bins, this gives an $\frac{87}{86}\text{Sr}$ isotopic ratio for the plagioclase population of 0.706217 ± 16

(with uncertainty contributions from each measurement within each bin weighted to the volume significance of each bin of the CSD as a fraction of the feldspar population), distinct from the whole rock at 0.706194 ± 12 . Groundmass glass was measured as 0.706184 ± 15 , lower than the whole-rock. Using the ICSD plot to inform our mass balance, we obtain a predicted whole-rock $\frac{87\text{Sr}}{86\text{Sr}}$ ratio of 0.706196 ± 16 , which is indistinguishable from the measured value.

6.3. Validity of the ICSD plot

As noted earlier, the formation of the ICSD plot hinges on key assumptions and criteria. Growth rates are difficult to measure directly, and these crystals all show evidence of resorption and regrowth. Any growth rate therefore has to be an average over a significant time interval. Moreover, there are at least two different isotopic signatures in the crystal cores, which must have been derived from different magmas either at the same time (in two different places) or different times (in possibly the same magma chamber). Therefore the hiatuses that have to be considered are significant. However, within the region of crystal growth that is preserved as crystal, the question is whether the mean crystal growth rate, during periods of accumulated, recorded growth, is constant. Work by Armienti et al. (2007) has shown that for the modern system at Stromboli this appears to be the case, and crystals record a mean growth rate of $2 \times 10^{-11} \text{ cm s}^{-1}$, consisting of a combination of peak growth rates of approximately $10^{-10} \text{ cm s}^{-1}$ coupled to significant resorption. The assumption that the crystals analysed represent the full crystallisation history is just that, an assumption, but one which does leave us with an essentially “correct” integrated isotopic ratio across all components. As mentioned earlier, this may be because such a test is quite insensitive to variations in crystal core size; however, it may also be because the technique is valid. Of greater concern is that the “oldest” point of the isotopic variation is held by only one zone in one crystal. In order to be able to assume that this is valid, we have another assumption, which is that the inherited cores followed a log-abundance vs. size relationship consistent with a normal CSD pattern, and that therefore our assumption that “larger crystals are older” is valid. As we have seen in the isotopic results alone, crystal rims need not be in equilibrium with their host melt. Therefore, smaller crystals could retain older, core-type isotopic signatures with no rim development. Short of analysing many more crystals in detail for their isotopic ratios, we cannot be certain that this parameter “averages out” in the way that growth rate variability may. Indeed, given

the time-consuming nature of the isotopic microsampling, it is highly unlikely that a more statistically significant sample set can be obtained through microdrilling. Laser-Ablation Multi-Collector Inductively Coupled Plasma Mass Spectrometry (LA-MC-ICPMS) may offer a route to obtaining data at higher rates, but the precision of the ratio determination is typically much worse than through microdrilling+TIMS. In systems displaying very large variations in isotopic contrast between crystal core and rim, this lower resolution may be acceptable, however for studies on Stromboli, it is not, as high precision in the isotopic analysis is pre-requisite to constructing a meaningful isotopic evolution line (Davidson et al., 2007).

More stringent tests of the ICSD concept are needed to determine if it is truly a viable technique. For the purposes of the current study, there appear to be only two major discontinuities recorded in the crystals, one following the generation of the core, and one leading to a loss of the final equilibrium rim. The ICSD generation process can cope with this level of variability. However it is difficult to assess the impact of variations in the initial population due to their lower abundance.

7. Implications for Stromboli Volcano

Fig. 6 shows that the change in isotopic ratio and kink in the CSD are coincident. Thus, the kink, representing the addition of an inherited crystal population and possible change in growth systematics, also represents the onset of transition to an isotopically distinct magma supply. The isotopic ratio of post-kink crystals changes continuously, representing magma mixing between newer and older magmas with their cargo of inherited feldspar crystals which become inherited cores in the final mixed product. These cores show minor isotopic variations which may represent earlier, smaller-scale contamination and mixing processes than the post-kink magma supply change. The post-kink phase of the CSD has a steeper gradient, suggesting either a crystal growth rate increase or mixing of two different crystal populations. Using the average growth rates determined as $2 \times 10^{-11} \text{ cm s}^{-1}$ for the modern Stromboli system (Armienti et al., 2007), and a slope for rim growth of -3.12 (in natural log terms), post-kink growth would take roughly 5 years. As this represents the time taken for the isotopic ratios to shift, this timescale also reflects the overturn and supply timescale of the magma chamber at Stromboli Volcano, and is consistent with the rates of isotopic shift observed in the modern system of ~ 19 years (Francalanci et al., 2005).

From earlier considerations of the isotopic variation and individual crystal histories, we can state that there were at least two sources of feldspar crystal core material (crystals STR461 and STR462 have distinct cores from STR463) that were introduced into an environment of changing magma composition. From the zonation of STR462, we can infer that it has been incorporated into a cumulate or mush zone of some type at least once to form the glomerocryst of cores, possibly a second time if the crystal does not actually record the final equilibrium melt composition (beyond our spatial resolution to test). From STR463 we can infer a similar history; crystallisation of the core in a reservoir distinct from that of STR461 and STR462 in either time or space, or both, with subsequent mobilisation into the changing reservoir and removal from the convecting magma, creating a definite hiatus at the crystal rim. Crystal STR461 appears to have shared much of its magmatic history with crystal STR462.

These crystal growth histories show that the magma system at Stromboli was highly dynamic during the Vancori period, and was particularly active during the initial period of isotopic ratio changes, where crystals were remobilised and kept in suspension. Convection gradually waned prior to eruption as crystals once more settled out of the convecting magma, before being remobilised in the eruption of STR46 itself. This kind of dynamic behaviour shows distinct similarities to the system of today, where crystal recycling and inheritance of crystal cores is a common process (Francalanci et al., 2005). The presence of distinct isotopic ratios in crystal cores shows that there was more than one inherited component, possibly from two distinct crystal mush lenses associated with different periods of activity. Furthermore, the timescales of isotopic variation in the Vancori period appear to have been quite similar to those of today, assuming that the same crystal growth rates operated in both cases.

The use of the isotopic evolution line to allow cross-comparison of crystal major element zonation appears to show that the major elements are not obviously correlated between crystals at points of common isotopic ratio, an observation also made elsewhere (Tepley et al., 2000). This may be due to one of several effects; variations in temperature, pressure and water fugacity across the magma chamber will affect the equilibrium composition of crystallising feldspar; similarly it is possible that crystal growth is associated with long periods of slow dissolution, and if these dissolution events are of varying extents, it has the potential to decouple crystal zonation patterns by variably erasing zonation patterns. Alternatively, highly localised kinetic

effects during crystal growth could generate chaotic zoning of major and trace elements whilst recording uniform isotopic ratios.

8. Conclusions

Our results suggest, from CSD and isotopic analysis, that there was a significant change in isotopic ratio at Stromboli volcano at the beginning of the Lower Vancori period. Using modern-system crystal growth rates as an analogue for the Vancori period, a timescale of the order of 5 years would be consistent with the CSD data and the accompanying isotopic shift. Combining the two datasets through an ICSD relation yields a quantitative isotopic evolution timeline for a magma system, a highly desirable result, useful for assessing magma supply changes, overturn, or crustal contamination events and the effects that these events have on crystal growth. The generation of a crystal timeline, by combining isotopic data to generate a common isotopic evolution trend, appears to be a powerful technique in itself. In this case, it allows some assessment of crystal inheritance mechanisms and magma dynamics, and also investigation of the homogeneity of crystallisation conditions during magma system evolution, although it necessitates the analysis of multiple (≥ 4) zones for isotopic ratio per crystal. The apparent variability of major element contents in crystal zones of comparable isotopic ratio suggests that either the crystallising environment was dynamic and heterogeneous with respect to some combination of temperature, pressure, water content and magma composition, or that very localised local kinetic effects control major element distributions during plagioclase crystallisation.

Acknowledgements

This work was sponsored by the EU 5th framework ERUPT project, EVG1-CT2002-00058. DM acknowledges support of Marie Curie fellowship MEIF-CT-2006-025204 during the preparation of the manuscript. The authors thank Chris Ottley for the assistance with the ICPMS measurements. The authors wish to thank Ariel Provost for a challenging and constructive review that has strengthened the manuscript markedly.

References

- Armienti, P., Francalanci, L., Landi, P., 2007. Textural effects of steady state behaviour of the Stromboli feeding system. *Journal of Volcanology and Geothermal Research* 160 (1–2), 86–98.
- Bindeman, I.N., Davis, A.M., Drake, M.J., 1998. Ion microprobe study of plagioclase-basalt partition experiments at natural concentration

- levels of trace elements. *Geochimica et Cosmochimica Acta* 62, 1175–1193.
- Boorman, S., Boudreau, A., Kruger, F.J., 2004. The lower zone–critical zone transition of the Bushveld Complex: a quantitative textural study. *Journal of Petrology* 45, 1209–1235.
- Cashman, K.V., Ferry, J.M., 1988. Crystal size distribution (CSD) in rocks and the kinetics and dynamics of crystallization III. Metamorphic crystallization. *Contributions to Mineralogy and Petrology* 99, 401–415.
- Cashman, K.V., Marsh, B.D., 1988. Crystal size distribution (CSD) in rocks and the kinetics and dynamics of crystallization II: Makaopuhi Lava Lake. *Contributions to Mineralogy and Petrology* 99, 292–305.
- Cashman, K.V., 1990. Textural constraints on the kinetics of crystallization of igneous rocks. In: Ribbe, P.H. (Ed.), *Modern Methods of Igneous Petrology — Understanding Magmatic Processes*. Reviews in Mineralogy, vol. 24. Mineralogical Society of America, pp. 259–314.
- Charlier, B.L.A., Wilson, C.J.N., Lowenstern, J.B., Blake, S., Van Calsteren, P.W., Davidson, J.P., 2005. Magma generation at a large, hyperactive silicic volcano (Taupo, New Zealand) revealed by U–Th and U–Pb systematics in zircons. *Journal of Petrology* 46, 3–32.
- Charlier, B.L.A., Ginibre, C., Morgan, D.J., N. G.M., Pearson, D.G., Davidson, J.P., Ottley, C.J., 2006. Methods for the microsampling and high-precision analysis of strontium and rubidium isotopes at single crystal scale for petrological and geochronological applications. *Chemical Geology* 232, 114–133.
- Davidson, J.P., Tepley III, F.J., 1997. Recharge in volcanic systems: evidence from isotope profiles of phenocrysts. *Science* 275, 826–829.
- Davidson, J.P., Morgan, D.J., Charlier, B.L.A., Harlou, R., Hora, J., 2007. Tracing magmatic processes and timescales through mineral-scale isotopic data. *Annual Reviews of Earth and Planetary Sciences* 35, 273–311.
- Ewart, A., Bryan, W.B., Gill, J.B., 1973. Mineralogy and geochemistry of the younger Volcanic Islands of Tonga, S. W. Pacific. *Journal of Petrology* 14, 429–465.
- Francalanci, L., Tommasini, S., Conticelli, S., Davies, G.R., 1999. Sr isotope evidence for short magma residence time for the 20th century activity at Stromboli volcano, Italy. *Earth and Planetary Science Letters* 167, 61–69.
- Francalanci, L., Tommasini, S., Conticelli, S., 2004. The volcanic activity of Stromboli in the 1906–1998 AD period: mineralogical, geochemical and isotope data relevant to the understanding of the plumbing system. *Journal of Volcanology and Geothermal Research* 131, 179–211.
- Francalanci, L., Davies, G.R., Lustenmhower, W., Mason, P., Tommasini, S., Conticelli, S., 2005. In-situ Sr-isotope microanalysis evidence of old crystal re-cycling and multiple magma reservoirs in the plumbing system of the present day activity at Stromboli, South Italy. *Journal of Petrology* 46, 1997–2021.
- Gagnevin, D., Daly, J.S., Poli, G., Morgan, D., 2005a. Microchemical and Sr isotopic investigation of zoned K-feldspar megacrysts: insights into the petrogenesis of a plutonic system and disequilibrium processes during crystal growth. *Journal of Petrology* 46, 1689–1724.
- Gagnevin, D., Daly, J.S., Waight, T.E., Morgan, D., Poli, G., 2005b. Pb isotopic zoning of K-feldspar megacrysts determined by laser ablation multiple-collector ICP-MS: insights into granite petrogenesis. *Geochimica et Cosmochimica Acta* 69, 1899–1915.
- Ginibre, C., Kronz, A., Worner, G., 2002. High-resolution quantitative imaging of plagioclase composition using accumulated back-scattered electron images: new constraints on oscillatory zoning. *Contributions to Mineralogy and Petrology* 142, 436–448.
- Higgins, M.D., 2000. Measurement of crystal size distributions. *American Mineralogist* 85, 1105–1116.
- Higgins, M.D., 1994a. Determination of crystal morphology and size from bulk measurements on thin sections: numerical modelling. *American Mineralogist* 79, 113–119.
- Higgins, M.D., 1994b. Numerical modeling of crystal shapes in thin-sections — estimation of crystal habit and true size. *American Mineralogist* 79, 113–119.
- Hornig-Kjarsgaard, I., Keller, J., Koberski, U., Stadlbauer, E., Francalanci, L., Lenhart, R., 1993. Geology, stratigraphy and volcanological evolution of the island of Stromboli, Aeolian arc, Italy. *Acta Vulcanologica* 3, 21–68.
- Jerram, D.A., Cheadle, M.C., Philpotts, A.R., 2003. Quantifying the building blocks of igneous rocks: are clustered crystal frameworks the foundation? *Journal of Petrology* 44, 2033–2051.
- Jerram, D.A., Kent, A., 2006. An overview of modern trends in petrography: textural and microanalysis of igneous rocks. *Journal of Volcanology and Geothermal Research* 154 (Introduction).
- Marsh, B.D., 1988. Crystal size distribution (CSD) in rocks and the kinetics and dynamics of crystallization I. Theory. *Contributions to Mineralogy and Petrology* 99, 277–291.
- Marsh, B.D., 1998. On the interpretation of crystal size distributions in magmatic systems. *Journal of Petrology* 39, 553–599.
- Mock, A., Jerram, D.A., 2005. Crystal size distributions (CSD) in three dimensions: insights from the 3D reconstruction of a highly porphyritic rhyolite. *Journal of Petrology* 46, 1525–1541.
- Morgan, D.J., Jerram, D.A., 2006. On estimating crystal shape for crystal size distribution analysis. *Journal of Volcanology and Geothermal Research* 154, 1–7.
- Muller, W., 2003. Strengthening the link between geochronology, textures and petrology. *Earth and Planetary Science Letters* 206, 237–251.
- Ramos, F.C., Wolff, J.A., Tollstrup, D.L., 2004. Measuring Sr-87/Sr-86 variations in minerals and groundmass from basalts using LA-MC-ICPMS. *Chemical Geology* 211, 135–158.
- Ramos, F.C., Wolff, J.A., Tollstrup, D.L., 2005. Sr isotope disequilibrium in Columbia River flood basalts: evidence for rapid shallow-level open-system processes. *Geology* 33, 457–460.
- Tepley III, J., Davidson, J.P., Tilling, R.I., Arth, J.G., 2000. Magma mixing, recharge and eruption histories recorded in plagioclase phenocrysts from El Chichon Volcano, Mexico. *Journal of Petrology* 41, 1397–1411.
- Tepley III, F.J., Davidson, J.P., 2003. Mineral-scale Sr-isotope constraints on magma evolution and chamber dynamics in the Rum layered intrusion, Scotland. *Contributions to Mineralogy and Petrology* 145, 628–641.
- Turner, S.P., George, R., Jerram, D.A., Carpenter, N., Hawkesworth, C.J., 2003. Case studies of plagioclase growth and residence times in island arc lavas from Tonga and the Lesser Antilles, and a model to reconcile discordant age information. *Earth and Planetary Science Letters* 214, 279–294.
- Wallace, G.S., Bergantz, G.W., 2002. Wavelet-based correlation (WBC) of zoned crystal populations and magma mixing. *Earth and Planetary Science Letters* 202, 133–145.
- Wallace, G.S., Bergantz, G.W., 2004. Constraints on mingling of crystal populations from off-center zoning profiles: a statistical approach. *American Mineralogist* 89, 64–73.
- Wolff, J.A., Ramos, F.C., 2003. Pb isotope variations among Bandelier Tuff feldspars: no evidence for a long-lived silicic magma chamber. *Geology* 31, 533–536.
- Zieg, M.J., Marsh, B.D., 2002. Crystal size distributions and scaling laws in the quantification of igneous textures. *Journal of Petrology* 43, 85–101.